LIGHT-WATER REACTOR PHYSICS PARAMETERS FOR TRANSIENT ANALYSIS

by

Jaime Olmos and K. F. Hansen

Energy Laboratory Report No. MIT-EL 75-022

June 1975

LIGHT-WATER REACTOR PHYSICS PARAMETERS FOR TRANSIENT ANALYSIS

by

Jaime Olmos

and

K. F. Hansen

Energy Laboratory

and

Department of Nuclear Engineering

Massachusetts Institute of Technology

Cambridge, Massachusetts 02139

Final Report for Task #1 of the Nuclear Reactor Safety Research Program

sponsored by

New England Electric System

Northeast Utilities Service Co.

under the

MIT Energy Laboratory Electric Power Program

Energy Laboratory Report No. MIT-EL 75-022

June 1975

Abstract

The nature and characteristics of nuclear reactor transients induced by control rod motions are important to light-water reactor safety analyses. Rod motion influences both local neutron absorption rates and the local neutron spectra. Studies on specific systems suggest that accurate prediction of transients requires that both the absorption rate change and the spectral change are necessary to represent control rod motion.

Contents

1. Introduction

The objective of this project has been to study means of representing few-group physics constants for control rod motion in reactor transients.

The main effect of rod motion is to change local thermal neutron absorption rates. However, due to spectral effects, all few-group parameters change as rods move into or out of an homogenized region. If all few-group parameters must be changed during reactor transients then computing costs of transient problems will be quite high. Further, knowing the reactivity worth of a control rod would not be sufficient information to predict the effects of rod ejection accidents.

An alternative procedure is to attempt to model the rod motion as a simple change in thermal absorption cross section. This is the simplest procedure to follow and also permits a means of representing control rod motion if the rod worth is known.

In this study a number of transient calculations have been made to compare results of calculations with complete or simple representations of the control rods. We have considered two different rod control cluster (R.C.C.) withdrawal problems, corresponding to reactivity insertions of \$1.906 and \$.896 respectively. We have used three different approaches for both problems. In the first (benchmark) case all the few-group parameter changes necessary to represent a R.C.C. withdrawal were included. In the second case only the thermal capture

cross section was changed by its correct amount while all the other parameters were left untouched. Notice however, that for this case the reactivity change did not correspond to the benchmark case. Finally, our third case consisted in changing only the thermal capture cross-section by an amount such that the reactivity insertion would correspond to the benchmark case.

2. Control Rod Representation

Initially it was planned to use the control cluster of an actual PWR for a test case. In which case the rod composition is a mixture of Ag(80%), In(15%) and Cd(5%). However, the multigroup cross-sections for these materials are not available in the LEOPARD[1] library. (LEOPARD is the spectrum code we have used to generate the few-group constants that represent pin-cells within a PWR assembly.) Instead we have considered our control rods to be made out of Hafnium, a material which closely resembles the actual rod nuclear properties. Though the Hafnium multigroup cross-sections are not readily available in LEOPARD, we have nevertheless found its multigroup thermal cross-section data present in the TEMPEST[2] library, while its multigroup non-thermal cross-section data were found in the MUFT library supplied by A. F. Henry[3].

The procedure used for finding the few-group rodded assembly parameters was the following:

Step 1.- LEOPARD was used to find the few-group constants for fueled pin-cells.

Step 2.- The average multigroup fluxes for fueled pin cells found by LEOPARD were used in conjunction with the ABH[4] method to predict the multigroup fluxes within a Hafnium pin.

Step 3.- The Hafnium pin few-group constants were found by collapsing the multigroup flux weighted cross-sections.

Step 4.- The rodded assembly cross-sections were found by performing a CITATION[5] few-group, space-dependent diffusion theory calculation and then flux weighting the few-group pin-cell constants.

STEP 1.

We input the data necessary to describe a 2.25 w/o fueled pin in the Zion-I reactor[6] and made the appropriate modifications in the LEOPARD code necessary to obtain an edit of the thermal and non-thermal multigroup fluxes.

DATA:

	Composition		
Volume % in:	pellet	clad	moderator
UO_2	100%		
(Zircaloy) Zr-2		100%	
H_2O			99.2163%
(Inconel) Ni			.4075%
(Inconel) Fe			.1802%
(Inconel) Cr			.1959%

Trace Elements

B-10 2000 ppm

Resonance temperature (°F)		1440
Pellet temperature		1445
Clad temperature		622
Moderator temperature		564.8
Buckling (cm^{-2})		.000274
Pellet (outer radius)	O.R. (in.)	.18295
Clad	O.R. (in.)	.211
Pitch (in.)		.563
Clad thickness (in.)		.0243
H_2O pressure (psia)		2250.
UO_2 density (g/cc)		10.3

We have for LEOPARD that the thermal and non-thermal groups are subdivided into 172 and 54 multigroups respectively (see Tables 1 and 2). In Figs. 1 and 2 we have sketched the shapes of the thermal and epithermal & fast multigroup fluxes as computed by the LEOPARD code.

Figure 1. Thermal Flux Spectrum

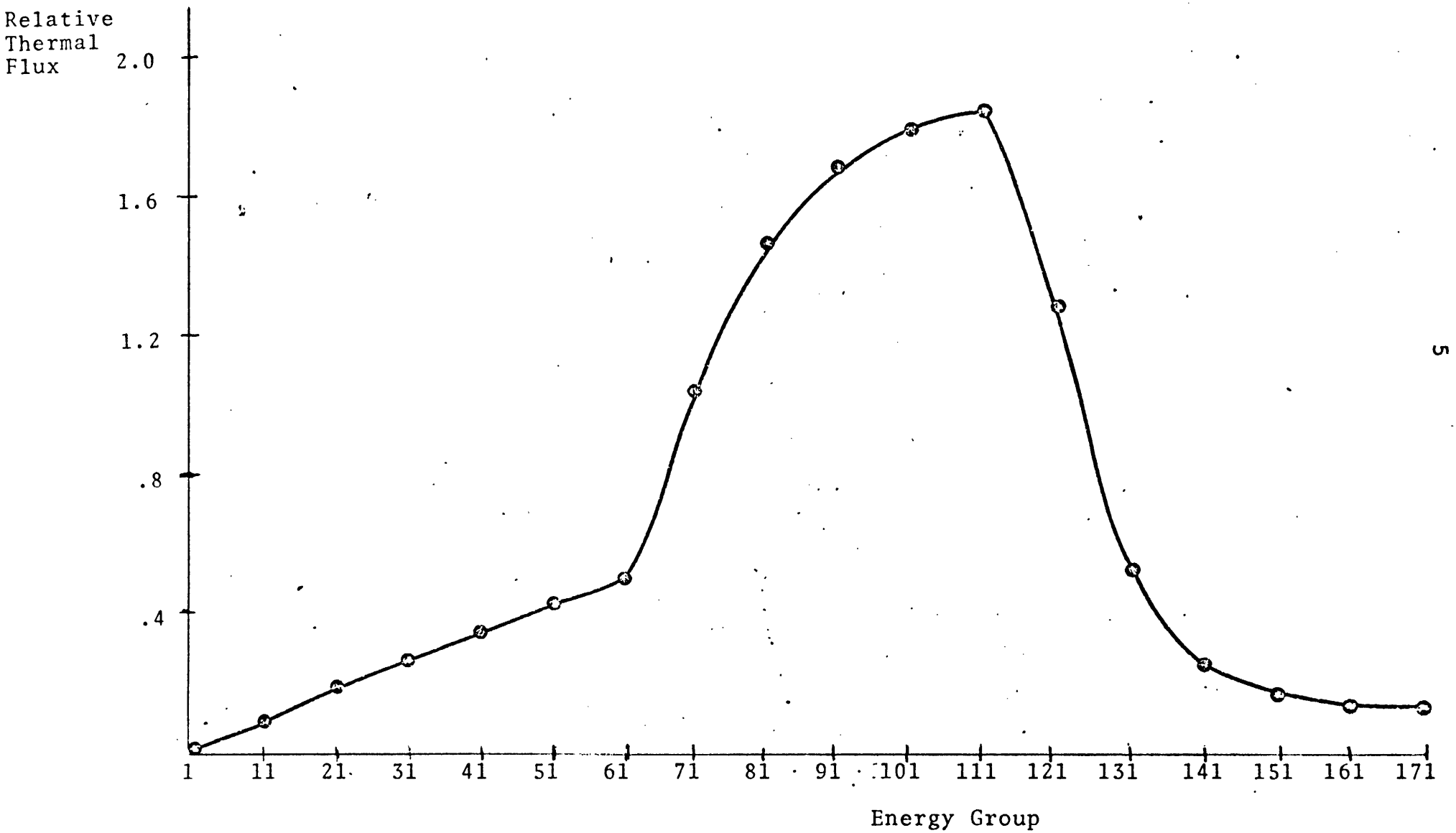

Figure 2. Epithermal and Fast Spectrum

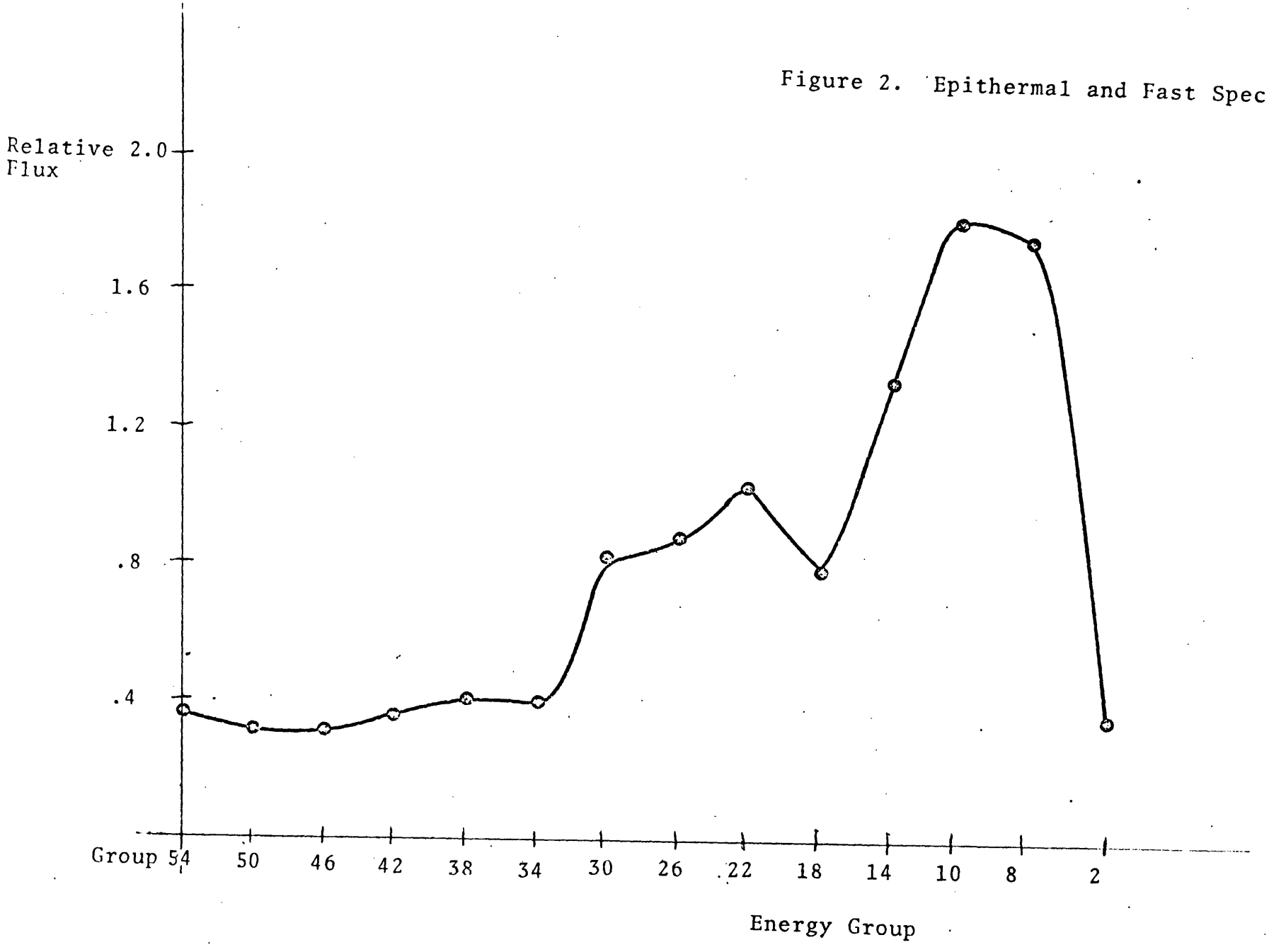

Table 1
Group Structure in LEOPARD

$$E(J) = \frac{J-1}{10^4} \quad \text{ev} \quad J = 1,161$$

$$\left(\text{i.e. } E(1) = 0,\ E(2) = \frac{1}{10^4},\ E(3) = \frac{2}{10^4},\ \ldots\ldots,\ E(61) = \frac{60}{10^4}\right)$$

$$E(J) = \frac{J-55}{10^3} \quad \text{ev} \quad J = 62,\ 115$$

$$\left(\text{i.e. } E(62) = \frac{7}{10^3},\ E(63) = \frac{8}{10^3},\ \ldots\ldots,\ E(115) = \frac{60}{10^3}\right)$$

$$E(J) = \frac{J-109}{10^2} \quad \text{ev} \quad J = 116,\ 172$$

$$\left(\text{i.e. } E(116) = \frac{7}{10^2},\ E(117) = \frac{8}{10^2},\ \ldots\ldots\ E(172) = \frac{63}{10^2}\right)$$

Table II

Group Structure in LEOPARD Library

Group Number	Energy (ev)	Lethargy	Lethargy Width
0	10×10^6	0	
1	7.79	0.25	0.25
2	6.07	0.50	
3	4.72	0.75	
4	3.68	1.00	
5	2.86	1.25	
6	2.23	1.50	
7	1.74	1.75	
8	1.35	2.00	
9	1.05	2.25	
10	821×10^3	2.50	
11	639	2.75	
12	498	3.00	
13	387	3.25	
14	302	3.50	
15	235	3.75	
16	183	4.00	
17	143	4.25	
18	111	4.50	
19	86.5	4.75	
20	67.4	5.00	0.25
21	40.9	5.50	0.50
22	24.8	6.00	
23	15.0	6.50	
24	9.12	7.00	
25	5.53	7.50	
26	3.35	8.00	
27	2.03	8.50	0.50
28	1.23	9.00	0.50
29	750×10^0	9.50	
30	454	10.00	
31	275	10.50	
32	167	11.00	0.50
33	130	11.25	0.25
34	101	11.50	
35	78.7	11.75	
36	61.3	12.00	
37	47.8	12.25	
38	37.2	12.50	
39	29.0	17.75	
40	22.6	13.00	
41	17.6	13.25	
42	13.7	13.50	
43	10.7	13.75	
44	8.32	14.00	
45	6.50	14.25	
46	5.10	14.50	
47	3.97	14.75	
48	3.06	15.00	
49	2.38	15.25	
50	1.855	15.50	0.25
51	1.440	15.7538	0.2538
52	1.125	16.00	0.2462
53	0.835	16.30	0.3000
54	0.625	16.5884	0.2884

STEP 2

We have estimated the multigroup fluxes inside a Hafnium pin by computing the disadvantage factors as predicted by the A.B.H. theory and by assuming the fluxes outside the Hafnium rod to be the same as the average fueled pin-cell multigroup fluxes obtained before.

Let $\Delta g \equiv$ group disadvantage factor

$\phi_R^g \equiv$ Hafnium rod group flux

$\phi_m^g \equiv$ Hafnium pin cell moderator flux

but by our assumption

$\phi_m^g \simeq$ Fueled pin cell average flux

then $\phi_R^g = \frac{\phi_m^g}{\Delta g}$ $g = 1, \ldots, G$

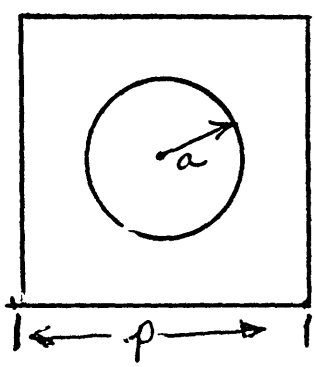

Fig. 3 Unit Pin - Cell

Let $f \equiv$ "group" utilization, $P_R \equiv$ "pin" escape probability

$P_m \equiv$ moderator escape probability.

$a \equiv$ rod radius, $H \equiv$ pin length, $S_R \equiv$ rod surface, $p \equiv$ pitch.

Then $V_R = \pi a^2 H$, $V_m = p^2 H - V_R$, $S_R = 2\pi a H$.

(Σ_a = absorption macroscopic cross-section)

(Σ_t = total macroscopic cross-section, Σ_s = scattering macroscopic cross-section)

The expression for the disadvantage factor is

$$\Delta_g = \frac{\phi m^g}{\phi_R^g} = \frac{\Sigma_{aR}\, V_R}{\Sigma_{am}\, V_m} \left(\frac{1}{f} - 1\right)$$

With

$$\frac{1}{f} - 1 = \frac{\Sigma_{am}\, V_m}{\Sigma_{aR}\, V_R} \frac{1}{P_R} + \frac{1-P_m}{P_m} - 4\frac{\Sigma_{am} V_m}{S_R}$$

with the escape probabilities given by

$$\frac{1}{P_R} = 1 + \left(\frac{\Sigma_{aR}}{\Sigma_{tR}}\right)\{A[1 + \alpha\left(\frac{\Sigma_{sR}}{\Sigma_{tR}}\right) + \beta\left(\frac{\Sigma_{sR}}{\Sigma_{tR}}\right)^2 + a\Sigma_{tR}]\}$$

$$\frac{1}{P_M} = \frac{V_m(ad)}{2V_R L_m^2} + E\,(\kappa_m a,\ \kappa_m b)$$

$$\kappa_m^2 = \frac{1}{L_m^2} = \frac{\Sigma_{am}}{D_m} \quad \text{and} \quad \pi b^2 = p^2$$

where $A = \dfrac{1 - P_{RO}}{P_{RO}} - a\Sigma_{tR}$

and P_{RO}, α and β are tabulated functions of $a\Sigma_{tR}$, while d is a tabulated function of the rod radius a and $E(\kappa ma, \kappa mb)$ is the lattice function for a cylindrical pin-cell rod.

Thus

$$\Delta_g = 1 + \left(\frac{\Sigma_{aR}}{\Sigma_{tR}}\right)\{A[1 + \alpha\left(\frac{\Sigma_{sR}}{\Sigma_{tR}}\right) + \beta\left(\frac{\Sigma_{sR}}{\Sigma_{tR}}\right)^2]\}$$

$$-a\Sigma_{aR} - \frac{\Sigma_{aR}\, V_R}{\Sigma_{am}\, V_m} + \frac{\Sigma_{aR}}{\Sigma_{am}} \left(\frac{ad}{2L_m^2}\right) + E(\kappa_m a,\ \kappa_m b) \frac{\Sigma_{aR}\, V_R}{\Sigma_{am}\, V_m}$$

(For convenience we have omitted the g-subscript from all our multigroup parameters)

Figs. 4 and 5 are sketches of the computed values for the thermal and non-thermal multigroup disadvantage factors.

STEP 3. We found the few-group constants which describe the Hafnium rods considered by performing the flux weighted sum of the values given for the multigroup cross-sections by the TEMPEST and MUFT libraries. We have

$$\overline{\Sigma_n^{Hf}} = \frac{\sum_{gcn} \phi_R^g \Sigma_{Hf}^g}{\sum_{gcn} \phi_R^g} \qquad n=1,2$$

($\sum_{gcn}$ indicates the sum over g = 1, ..., G for the multigroups contained in n, i.e. g = 1, ..., 172 for n = 2 and g = 1, ..., 54 for n = 1. n = 1 corresponds to the non-thermal group and n = 2 corresponds to the thermal group.)

The results obtained were the following:

(c ≡ capture, tr ≡ transport)

$$\bar{\Sigma}_{c_1}^{Hf} = .0408 \text{ cm}^{-1} \; ; \; \bar{\Sigma}_{tr1}^{Hf} = .3395 \text{cm}^{-1}$$

$$\bar{\Sigma}_{c_2}^{Hf} = 4.13 \text{ cm}^{-1} \; ; \; \bar{\Sigma}_{tr2}^{Hf} \quad 4.489 \text{cm}^{-1}$$

(We have neglected the scattering transfer cross-section $\bar{\Sigma}_{1\to2}^{Hf}$ inside the Hafnium rod.)

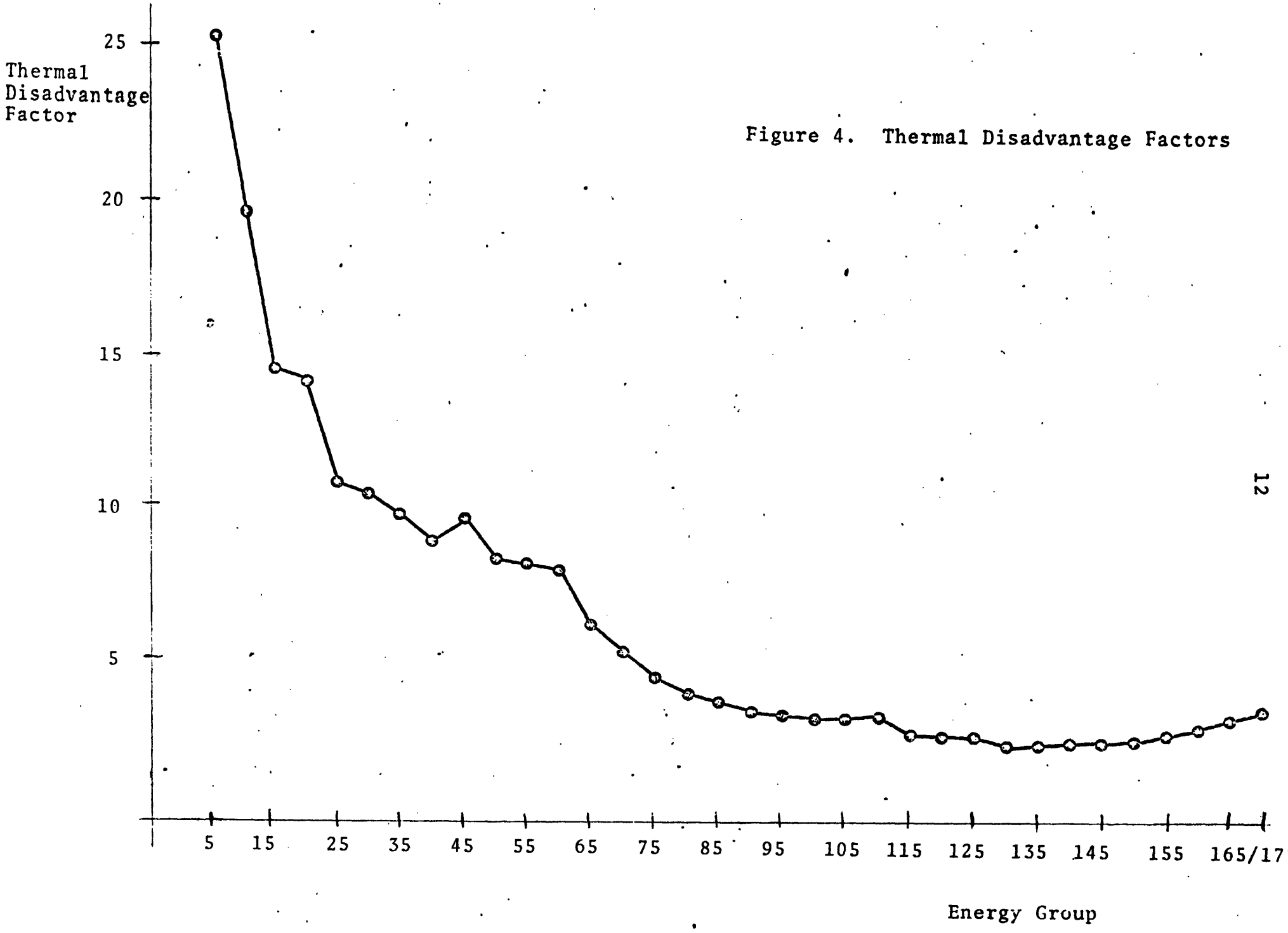

Figure 4. Thermal Disadvantage Factors

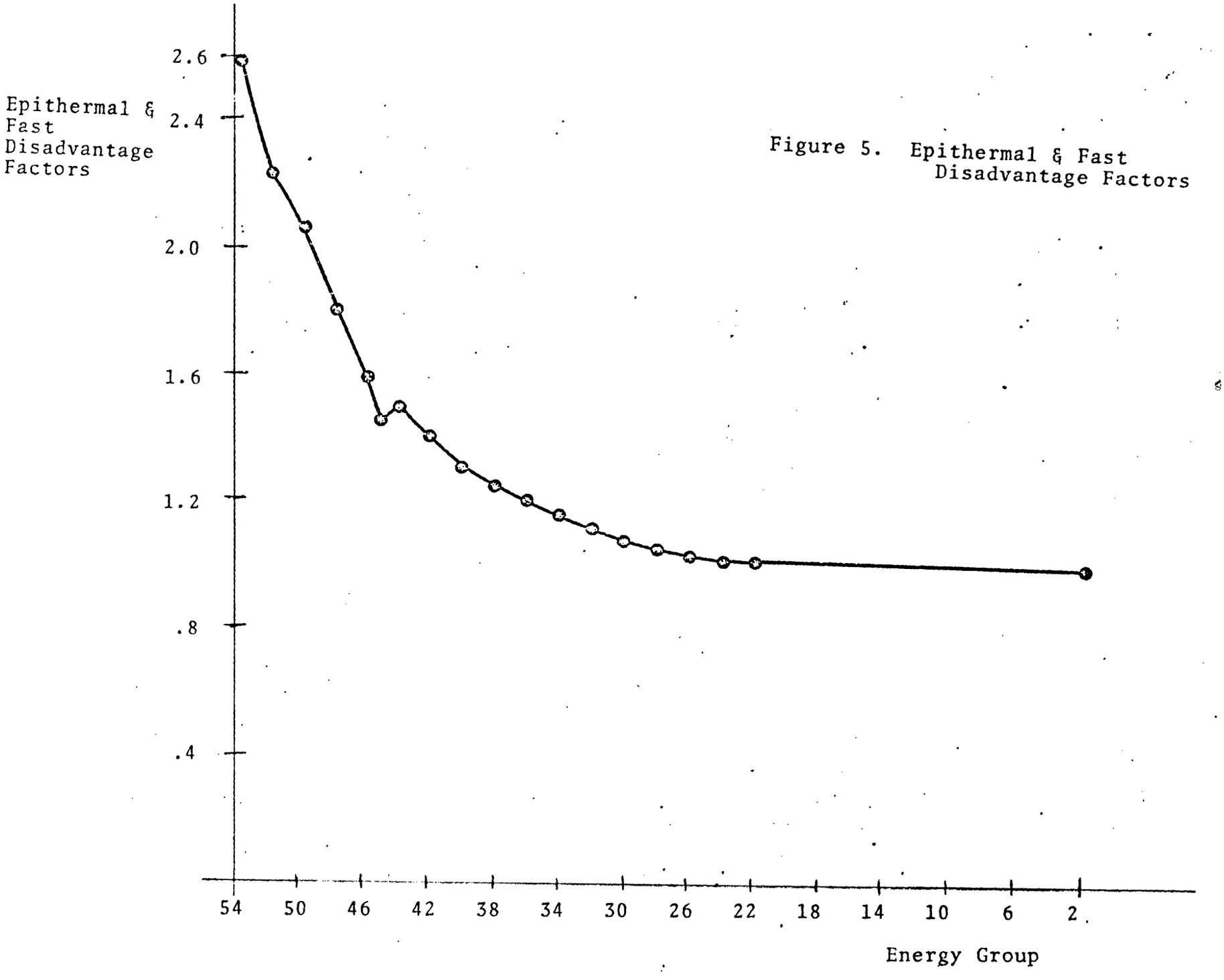

Figure 5. Epithermal & Fast Disadvantage Factors

STEP 4. We have used the CITATION code to generate equivalent two-group cross-sections that will represent homogenized assemblies in the Zion-I reactor. In particular we have considered three different enrichments (2.25 w/o, 2.8 w/o and 3.3 w/o) for the unrodded assemblies, while we have taken the Hafnium R.C.C. assemblies to have a 2.25 w/o enrichment.

We list here the data necessary to describe the PWR Zion-I assemblies considered:

Fuel Assemblies	
Rod array	15 X 15
Fuel-Rods per assembly	204
Rod pitch (in.)	.563
Overall dimensions (in.)	8.426 X 8.426
Number of Zr-2 Guide Thimbles	20
Rod Control Cluster Assemblies	
Neutron Absorber	H_f
Cladding Material	SS-304
Clad thickness (in.)	.019
Number of control rods per cluster	20

Figure 6 illustrates the geometry of an assembly. The crossed pins are unfueled in the case of fuel assemblies (i.e. they are filled with water) while for the case of an R.C.C. assembly these are to be the locations containing Hafnium (all except for one at the center which is used for instrumentation purposes).

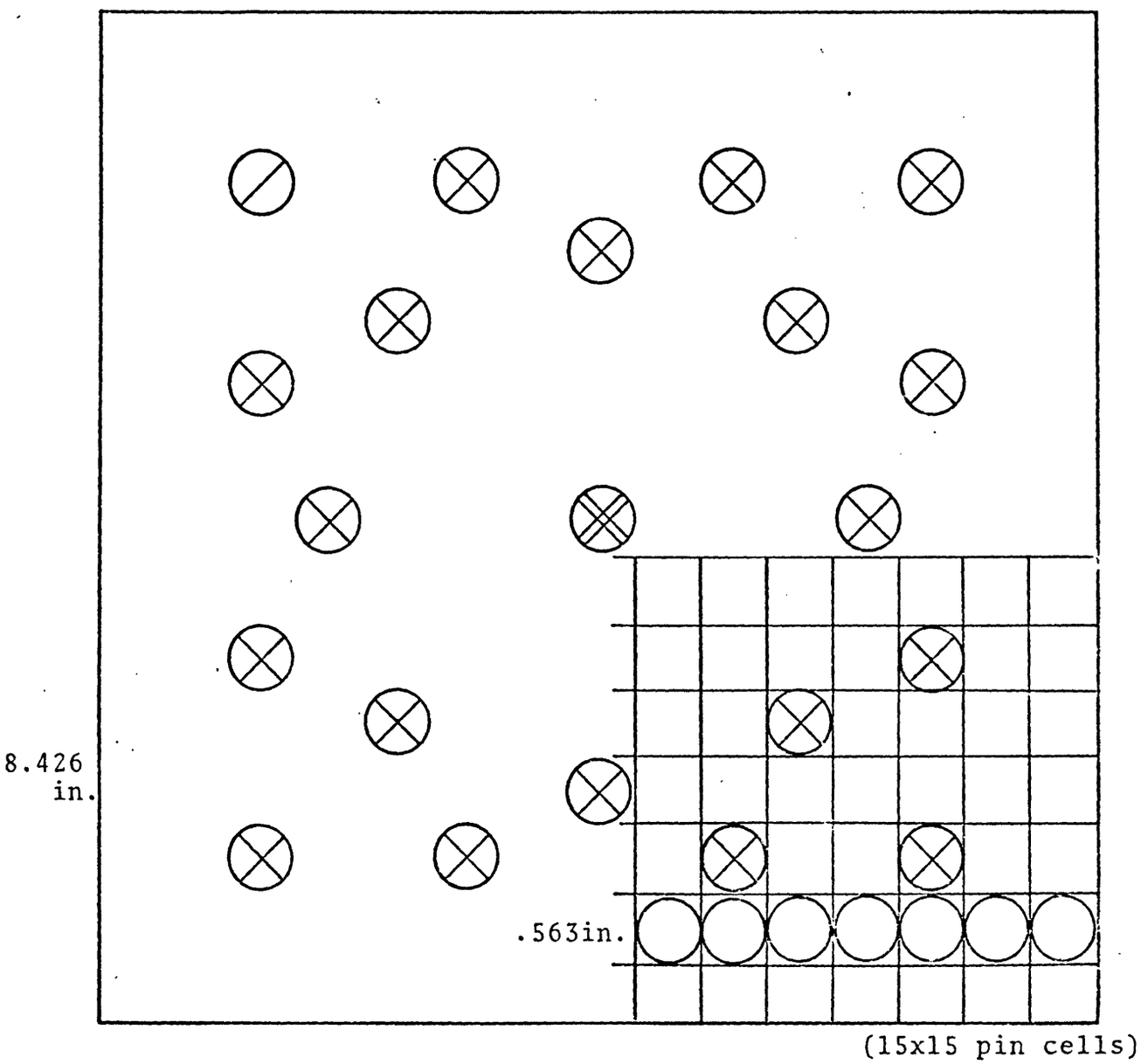

Figure 6 PWR Zion-I assembly profile

The two-group assembly cross-section values found for the different cases considered are as follows:

3.3 w/o enriched fuel assembly:

	Group 1	Group 2
Σ_f	2.636×10^{-3}	5.708×10^{-2}
Σ_c	7.211×10^{-3}	4.618×10^{-2}
Σ_{tr}	2.326×10^{-1}	8.937×10^{-1}
$\Sigma(1\rightarrow2)$	1.682×10^{-2}	

2.8 w/o enriched fuel assembly:

	Group 1	Group 2
Σ_f	2.381×10^{-3}	4.980×10^{-2}
Σ_c	7.184×10^{-3}	4.529×10^{-2}
Σ_{tr}	2.320×10^{-1}	8.916×10^{-1}
$\Sigma(1\rightarrow2)$	1.738×10^{-2}	

2.25 w/o enriched fuel assembly:

	Group 1	Group 2
Σ_f	2.091×10^{-3}	4.144×10^{-2}
Σ_c	7.157×10^{-3}	4.429×10^{-2}
Σ_{tr}	2.313×10^{-1}	8.890×10^{-1}
$\Sigma(1\rightarrow2)$	1.852×10^{-2}	

Hafnium R.C.C. (2.25 w/o enriched) assembly:

	Group 1	Group 2
Σ_f	2.093×10^{-3}	4.439×10^{-2}
Σ_c	8.406×10^{-3}	9.332×10^{-2}
Σ_{tr}	2.303×10^{-1}	8.949×10^{-1}
$\Sigma(1\rightarrow2)$	1.732×10^{-2}	

A comparison of the two-group parameters obtained for the 2.25 w/o enriched Hafnium rodded assembly with those obtained for the 2.25 w.o enriched unrodded assembly shows the thermal capture cross-section to be the parameter most affected. Its value has in fact increased by 210.7%. Ignoring fractional changes of less than 1% we find that the non-thermal capture cross-section has been increased by 17.45% while the scattering cross-section was decreased by 6.93%.

3. Rod Withdrawal Transient Calculation

Two one-dimensional sample problems were constructed in order to examine different approaches to simulate reactor transients involving a rod ejection. A one-dimensional profile of a PWR characteristic of the Zion-I reactor was used. The region compositions for the two sample problems are shown in figures 7 and 8. The outer regions are water reflectors, the 2nd and 14th regions are double thicknesses(2 assemblies) of 3.3 w/o enriched U-235.

Regions 3 and 13 have a full Hf rod cluster inserted in the 2.25 w/o enriched assemblies for problem 1, while they are only taken to be 1/2 inserted (as far as their overall effect on the few group parameters) for problem 2. Regions 7 and 9 have 1/4 inserted Hf R.C. Clusters for problem 1, while they are only 1/8 inserted for problem 2. These rod control cluster insertions have been so arranged in order to have relatively flat power distributions. The rest of the regions alternate between 2.25 w/o and 2.8 w/o enriched assemblies.

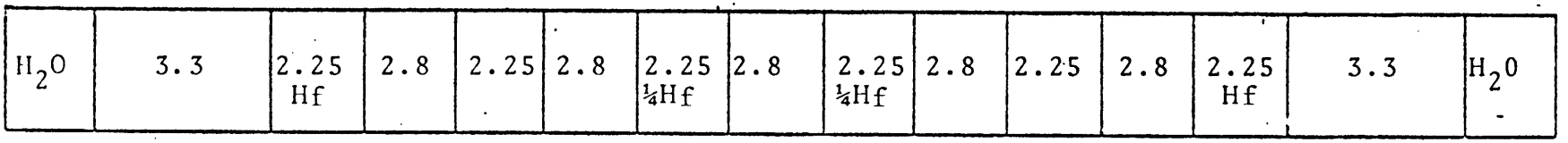

Region 1 2 3 4 5 6 7 8 9 10 11 12 13 14 15

Mesh pt. 1 6 16 21 26 31 36 41 45 51 56 61 66 71 81 86

Figure 7. One Dimensional PWR Core CrossSection (Problem 1)

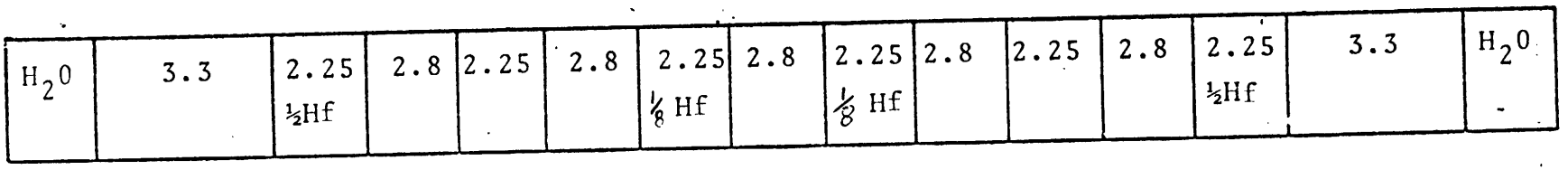

Region 1 2 3 4 5 6 7 8 9 10 11 12 13 14 15

Mesh pt. 1 6 16 21 26 31 36 41 45 51 56 61 66 71 81 86

Figure 8. One Dimensional PWR Core Cross Section (Problem 2)

Our 1- dimensional kinetics simulations have been done using the GAKIN-II[7] code, thus we have not taken into account feedback effects on our transients. For both problems 1 and 2 the partially rodded region #7 (1/4-Hf rodded for problem 1 and 1/8-Hf rodded for problem 2) experiences a rod control cluster ejection over a 1 second period. We can compute the final reactivity insertion after this one second period from knowledge of the effective multiplication factors (k_{eff}) for the system with region #7 rodded and unrodded. Thus the final reactivity insertion in dollars will be

$$\Delta\rho = \frac{1}{\beta}\left(1 - \frac{k_{eff}\ (\text{rodded})}{k_{eff}(\text{unrodded})}\right)$$

For problem 1, k_{eff} (unrodded) = .98894 and k_{eff} (rodded) = .97480, thus the rod worth here will be \$1.906 since the delayed fraction β is .0075. Problem 2 was constructed to consider a situation with a reactivity insertion below super-prompt critical. We have here k_{eff} (unrodded) = .99539 and k_{eff} (rodded) = .9887, so the rod worth here will be \$.896.

As mentioned in the introduction we have treated 3 cases for each of the two problems considered. In the first (benchmark) case we have changed linearly with time all the few-group parameters of region #7 over the one second period. In the second case only the thermal-group capture cross-section was changed, as this is the single parameter most affected by the rod motion. Here however the reactivity insertion does not coincide with the one for cases 1 and 3. In the third case we adjusted the thermal-capture cross-section change so as to make that single change of

parameter to cause the same reactivity insertion as for case one.

A sample of the results obtained in both problems is given in the tables below.

Table 3

Time dependent fluxes for benchmark case with all parameters varying linearly with time.

(Problem 1)

	t=0.0	t=0.1	t=0.2	t=0.3	t=0.4	t=0.5
Group 1						
Point						
10	1.2493	1.3420	1.4894	1.7182	2.1187	2.9560
20	.8900	.8925	1.0220	1.2234	1.5763	2.3176
40	1.487	1.7201	2.0708	2.6166	3.5737	5.5974
60	1.793	1.9219	2.1228	2.4358	2.9836	4.1299
80	.7224	.7535	.8042	.8828	1.020	1.3061
Group 2						
Point						
10	.2018	.2168	.2406	.2776	.3424	.4777
20	.1061	.1170	.1340	.1605	.2068	.3041
40	.2761	.3230	.3935	.5033	.6959	1.1035
60	.3826	.4100	.4529	.5197	.6367	.8814
80	.1268	.1323	.1412	.1550	.1792	.2294

Table 4

Time dependent Flux Ratios for Case 2, Thermal Capture Cross sections only varying, non-equivalent Δk.

(Problem 1)

	t=0.0	t=0.1	t=0.2	t=0.3	t=0.4	t=0.5
Group I						
Point						
10	1.0	.9964	.9901	.9796	.9607	.9226
20	1.0	.9951	.9871	.9746	.9530	.9120
40	1.0	.9929	.9826	.9675	.9433	.8997
60	1.0	.9965	.9905	.9803	.9618	.9241
80	1.0	.9978	.9937	.9865	.9726	.9408
Group 2						
Point						
10	1.0	.9965	.9903	.9797	.9606	.9226
20	1.0	.9953	.9873	.9744	.9530	.9120
40	1.0	.9922	.9813	.9654	.9406	.8964
60	1.0	.9966	.9905	.9804	.9617	.9240
80	1.0	.9981	.9940	.9868	.9721	.9408

Table 5

Time Dependent Flux ratios for Case 3, Thermal capture cross section only varying, equivalent Δk.

(Problem 1)

	t=0.0	t=0.1	t=0.2	t=0.3	t=0.4	t=0.5
Group 1						
Point						
10	1.0	1.0008	1.0024	1.0058	1.0127	1.0291
20	1.0	1.0011	1.0031	1.0072	1.0152	1.0332
40	1.0	1.0016	1.0043	1.0093	1.0185	1.0382
60	1.0	1.0007	1.0023	1.0055	1.0124	1.0286
80	1.0	1.0004	1.0015	1.0038	1.0092	1.0221
Group 2						
Point						
10	1.0	1.0009	1.0027	1.0059	1.0126	1.0291
20	1.0	1.0013	1.0034	1.0071	1.0152	1.0333
40	1.0	1.0015	1.0043	1.0092	1.0183	1.0379
60	1.0	1.0007	1.0024	1.0056	1.0124	1.0286
80	1.0	1.0007	1.0018	1.0041	1.0090	1.0222

Table 6

Time dependent fluxes for benchmark case with all parameters varying linearly with time.

(Problem 2)

	t=0.0	t=0.2	t=0.4	t=0.6	t=0.8	t=1.0
Group 1						
Point						
10	1.2665	1.4012	1.6340	2.0796	3.1694	7.9958
20	.9710	1.1030	1.3287	1.7597	2.8181	7.5560
40	1.6354	1.9781	2.5531	3.6485	6.3549	18.6904
60	1.6280	1.7975	2.0894	2.6475	4.0138	10.0798
80	.7149	.7630	.8475	1.0095	1.4037	3.1220
Group 2						
Point						
10	.2048	.2266	.2643	.3364	.5127	1.2934
20	.1591	.1807	.2177	.2884	.4618	1.2384
40	.3250	.3981	.5204	.7533	1.3292	3.9606
60	.3476	.3838	.4462	.5655	.8574	2.1534
80	.1256	.1341	.1490	.1774	.2467	.5488

Table 7

Time dependent flux ratios for case 2, thermal capture cross-sections only varying, non-equivalent Δk.

(Problem 2)

	t=0.0	t=0.2	t=0.4	t=0.6	t=0.8	t=1.0
Group 1						
Point						
10	1.0	.9952	.9860	.9675	.9236	.7880
20	1.0	.9940	.9833	.9626	.9160	.7784
40	1.0	.9913	.9776	.9537	.9038	.7647
60	1.0	.9953	.9863	.9680	.9243	.7883
80	1.0	.9968	.9903	.9759	.9382	.8084
Group 2						
Point						
10	1.0	.9953	.9860	.9675	.9236	.7880
20	1.0	.9939	.9833	.9625	.9161	.7785
40	1.0	.9906	.9762	.9514	.9010	.7617
60	1.0	.9954	.9863	.9680	.9243	.7883
80	1.0	.9970	.9900	.9761	.9384	.8083

Table 8

Time dependent flux ratios for case 3, thermal capture cross-section only varying, equivalent Δk.

(Problem 2)

	t=0.0	t=0.2	t=0.4	t=0.6	t=0.8	t=1.0
Group 1						
Point						
10	1.0	1.0016	1.0053	1.0137	1.0375	1.1366
20	1.0	1.0020	1.0062	1.0158	1.0413	1.1432
40	1.0	1.0029	1.0085	1.0198	1.0477	1.1532
60	1.0	1.0016	1.0051	1.0135	1.0372	1.1365
80	1.0	1.0011	1.0035	1.0101	1.0302	1.1229
Group 2						
Point						
10	1.0	1.0018	1.0053	1.0137	1.0375	1.1366
20	1.0	1.0022	1.0064	1.0157	1.0415	1.1432
40	1.0	1.0028	1.0083	1.0195	1.0474	1.1528
60	1.0	1.0017	1.0051	1.0135	1.0373	1.1365
80	1.0	1.0011	1.0033	1.0104	1.0304	1.1228

For both problems we have listed the group fluxes as predicted by the benchmark case (Tables 3 & 6) at the set of mesh points (10, 20, 40, 60, 80) for the times (t=0 sec., t=.1 sec., t=.2 sec., t=.4 sec., t=.6 sec., t=.8 sec., t=1 sec.) for problem 2. As shown in Figures 7 and 8 points 10 and 80 lie inside 3.3 w/o enriched outer regions, point 20 lies inside Hf-rodded region #7 which is to experience the R.C.C. ejection, and point 60 lies inside a 2.25 w/o enriched region.

The results obtained in our benchmark case for problems 1 and 2 are compared with cases 2 and 3 in tables 4, 5, 7, 8. In these tables we have computed the ratios of the two-group fluxes as predicted by cases 2 and 3 to the two-group fluxes given by the benchmark case.

We observe that while for problem 1, case 2 underpredicts the fluxes by as much as 10% at t=.5 sec., case 3 overestimates the fluxes only by 4%. Similarly for problem 2 we find that while case 2 underpredicts the fluxes by as much as 25% at t=1 sec., case 3 overestimates the fluxes only by 15%. Notice also how the error percent prediction for the thermal and non-thermal fluxes at the different space-time points nearly coincides in both cases 2 and 3 and for the two problems considered.

Figures 9 and 10 are sketches of how the thermal flux increases with time in problems 1 and 2.

4. Conclusions

We have found that the insertion of a Hafnium rod control cluster into a reactor assembly has as its main effect a considerable increase of the thermal capture cross-section value

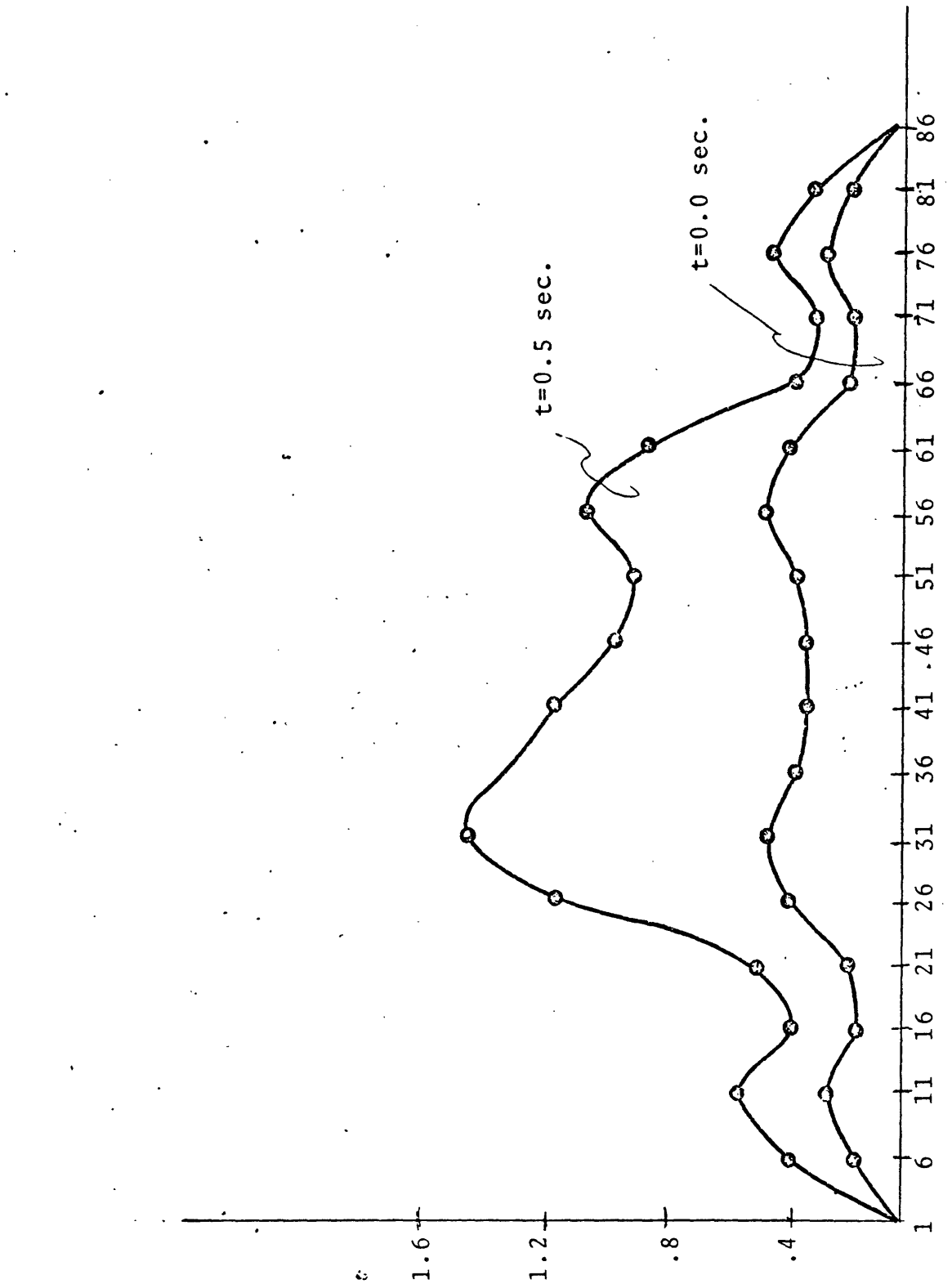

Figure 9. Time Dependent Thermal Fluxes (Problem 1)

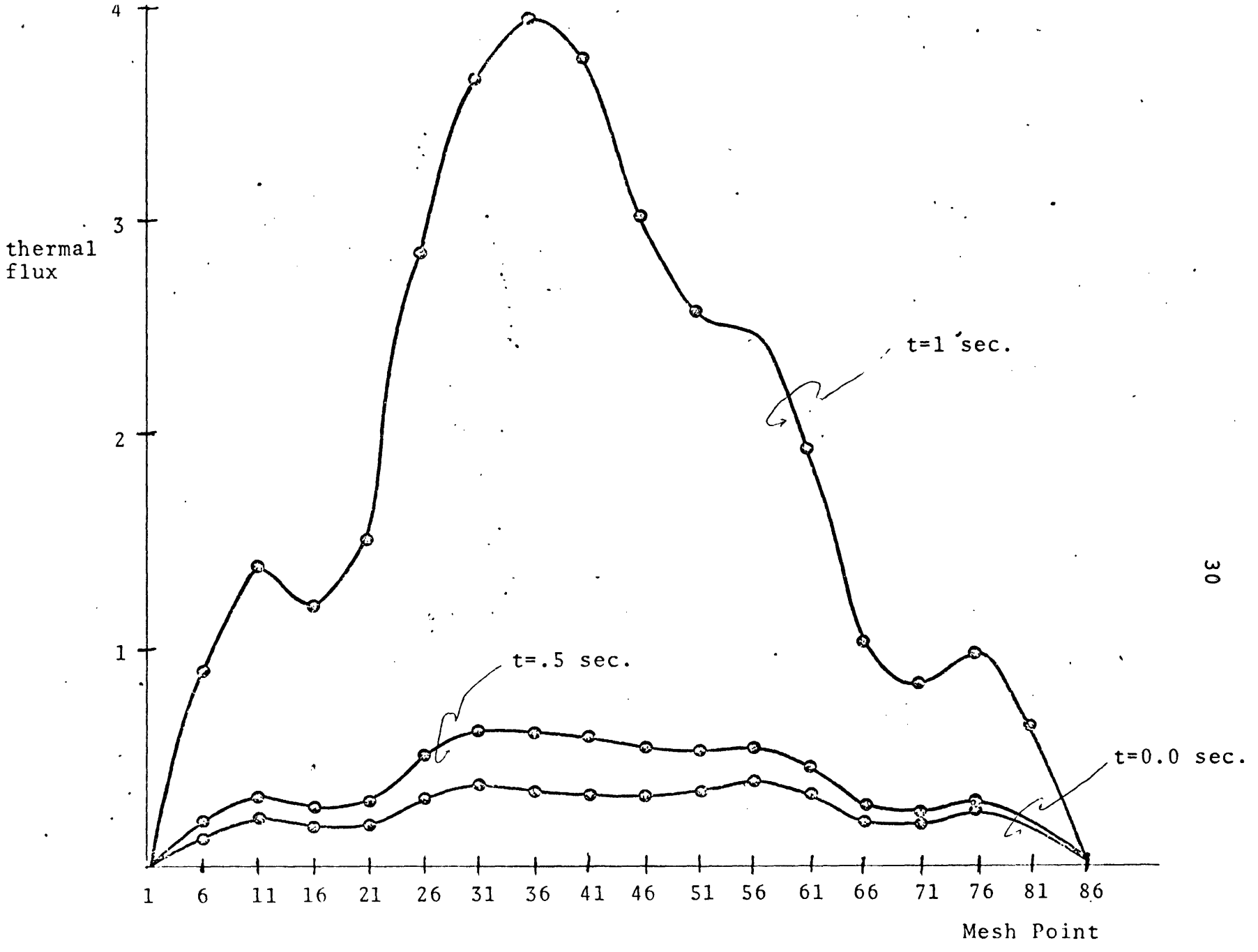

Figure 10.Time Dependent Thermal Fluxes (Problem 2)

associated with the homogenized parameters characterizing the assembly. This being the case we are naturally led to represent rod control cluster ejections by a simple change in the thermal capture assembly cross-section. The results obtained when using this approach in transient calculations are unacceptable as compared to accurate results where all few-group parameters are time dependent. The results are improved considerably if the thermal capture cross-section is artificially changed so as to preserve the total rod worth. Even in this case errors of 15% in power seem probable. Thus, it seems important to represent all time varying few-group parameters in transient analysis.

References

1. R. F. Barry, "LEOPARD - Spectrum dependent Non-spatial Depletion Code." WCAP-3269-26 (September 1963).

2. J. Dyer and R. H. Shudde, "TEMPEST, A Neutron Thermalization Code", NAA (September 1960).

3. A. F. Henry, "MUFT-1 Library", WAPD-TM-224

4. Lamarsh, J. R., Introduction to Nuclear Reactor Theory, (1966), Chapter 11.

5. T. B. Fowler et. al., NUCLEAR REACTOR ANALYSIS CODE: CITATION, ORNL-TM-2496 (July 1969).

6. Zion-I - Final Safety Analysis Report Vol. I, Commonwealth Edison Company.

7. Gakin II: "A One-dimensional Multigroup Diffusion Theory Reactor Kinetics Code," by J. H. Mason and K. F. Hansen (August 1973), MITNE-151.